Physics
UNIVERSITY OF TORONTO

PXR
Advanced Undergraduate Laboratory

Powder Methods of X-Ray Analysis

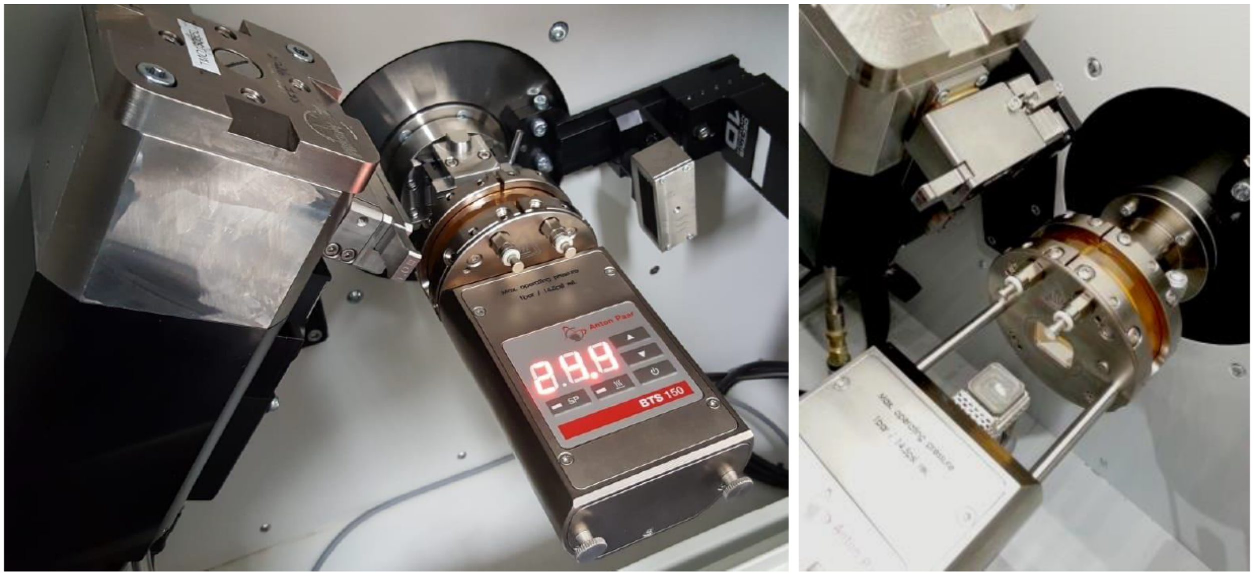

Revisions

2022-Sep	David Bailey & Lechun Xing
2014, 2021	David Bailey
1996	Bryan Statt

Contents

1 Introduction

X-ray diffraction by crystal was first demonstrated in 1912 by Max von Laue and W.L. Bragg in 1913. The use of powder in X-ray analysis was first demonstrated about 1916 when Debye and Scherrer in Germany and Hull in the United States independently obtained X-ray diffraction patterns from aggregates of microscopic crystals or powders (Barrett and Masssalski: Chapter 7 [1]). The method has proved of great importance. X-ray analysis provides information on the structure of crystalline materials. The overall structure as well as individual atomic positions can be determined.

Powder X-Ray (PXR) diffraction is capable of providing information about lattice constants in powder samples using a narrow, well collimated, monochromatic x-ray beam. In comparison, Laue X-ray diffraction uses a broadband x-ray beam to investigate crystal structures and orientations in single crystals.[1]

In a powder, each grain diffracts incident X-rays to generate diffraction peaks corresponding to some sets of crystal planes as the scattering angle 2θ is varied. (Note: A "powder" can be an actual powder or a polycrystalline solid sample such as a metal wire or sheet.) If the grains or tiny crystals are oriented at random, some of them will be set at the right angle to give a strong reflection, i.e. constructive interference of the diffracted rays, from a particular set of planes [2].

---

[1] If another student is doing the LAUE experiment, you may want to discuss collaborating to measure the same material (if available in polycrystalline and single crystal form) and comparing your results. Another interesting possible collaboration is with any HTCM students; you can study the crystal structure of their YBCO pellets and see if it is as expected.

Since the orientation is random in three dimensions the reflected X-rays from all the grains will lie on the surface of a cone of semi-vertical angle 2θ relative to the incident beam (Figure 1), where θ satisfies Bragg's law for the wavelength of the incident X-rays:

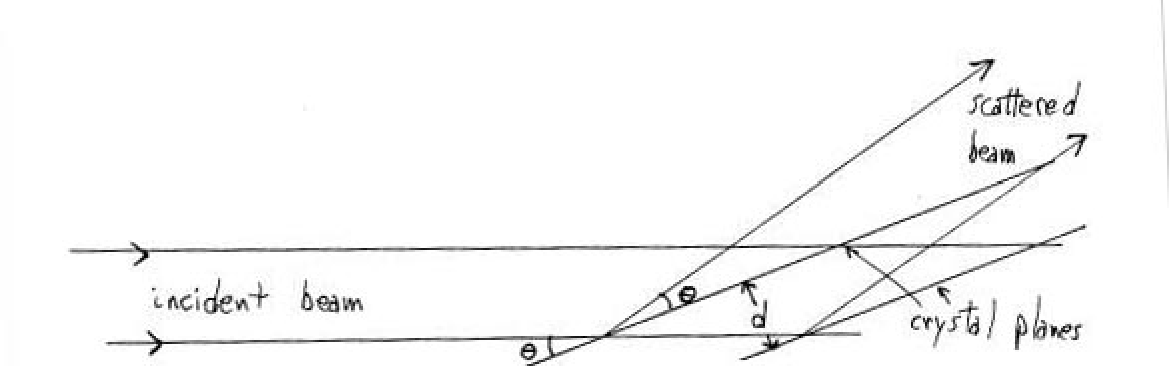

Figure 1: The cone referred to in the text (above) is generated by rotating the figure about the line of incidence of the X-rays. Note that the scattering angle in this figure is 2θ, twice the Bragg angle. Crystallographers depart strongly from researchers in other branches of physics who use the symbol θ to denote the angle through which the beam has been scattered.

$$n\lambda = 2d\sin\theta\,. \tag{1}$$

The Bragg condition (1) is a simple interference maximum, sharply defined when the number of parallel planes and their estimate is large.

Thus a monochromatic beam of X-rays passing through or reflecting from a finely divided powder will diffract x-rays in a series of concentric rings, each uniformly intense and corresponding to one set of planes of spacing d and one order of interference n. When a detector scans through these angles, these rings will show up as peaks in a spectrum, as shown in Figure 2. Substituting these in Bragg's equation, with the wavelength of the X-rays known from other information, a set of (d/n) values is obtained which may be used to determine the crystalline structure of the substance and its lattice parameters, or to identify the substance itself from the standard comparison values that are available.

Monochromatic X-rays are used in powder work because of the difficulty, if more than one wavelength is present in the beam, of determining which wavelength produced a given ring. The monochromatic X-rays are usually produced by exciting the K_α and K_β lines of a target in an evacuated X-ray tube. To remove the K_β lines, one can place in the external X-ray beam a filter of a material having an absorption edge of wavelength between the K_α and K_β of the target spectrum. This means that the filter is of an element one or two atomic numbers lower than the target in the X-ray tube; for example, a nickel filter is used with a copper target and a zirconium filter with a molybdenum target. (See Barrett [1], Chapter 3).

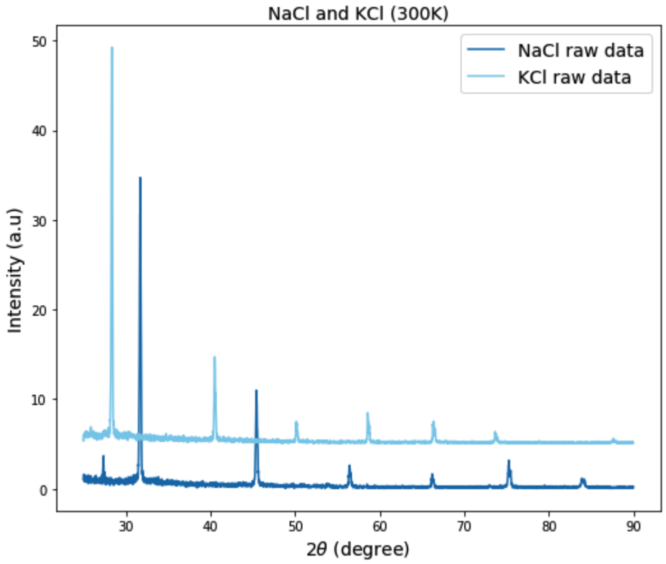

Figure 2: Comparing NaCl and KCl spectra at room temperature.

2 Experimental setup

X-rays ($0.1\mathring{A} \leq \lambda \leq 100\mathring{A}$) have wavelengths of the same order as atomic and molecular lattice constants. High quality diffraction patterns can be achieved with high intensity and monochromatic gratings. In this experiment, a narrow, well collimated, quasi-monochromatic X-ray beam is used, similar to that in Figure 4.

2.1 X-ray tube

X-rays are commonly produced in evacuated tubes by thermal emission electrons from a hot cathode that are accelerated by a voltage difference between the cathode and a target anode. When the electrons hit the anode, a broad spectrum of x-rays is produced by bremsstrahlung ("braking radiation"), and narrow peaks are produced by the fluorescence of target atoms excited by the electrons. The maximum x-ray energy is set by the accelerating voltage between the the cathode and anode, e.g. if the accelerating voltage is 25 KV, the maximum x-ray energy is 25 KeV. The current is the tube corresponds to the rate of electrons per second flowing from cathode to anode.

3 Theory and Interpretaion

The is not an exhaustive introduction to crystal structure. A full understanding of X-ray diffraction requires study of the concept of reciprocal lattice, and the reciprocal lattice vectors, **G** [1], [3]. The recommended reading list from the instrument's manufacturer is also a useful resource.

The set of reciprocal lattice vectors determine the possible X-ray reflections, the condition

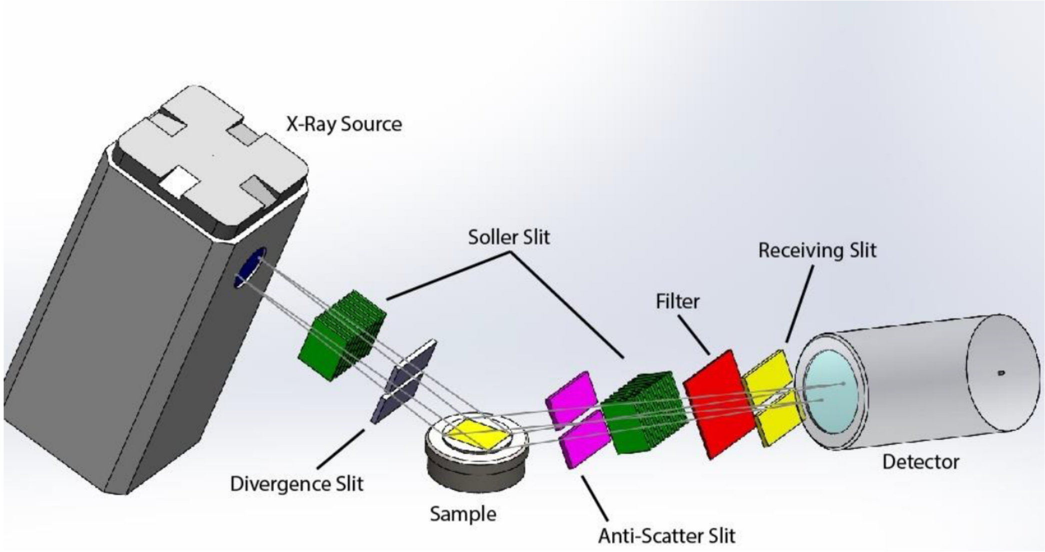

Figure 3: Schematic sketch of the setup, θ is measured between the X-ray primary beam and the sample, while 2θ is measured between the reflected beam and the transmitted primary beam.

being

$$2\vec{k} \cdot \vec{G} = G^2 \,, \tag{2}$$

which is equivalent to the Bragg condition 1. For cubic crystals there is only one lattice constant: a, the length of the edge of the unit cell. The spacing, d, between adjacent atomic planes is related to the lattice constant by the formula

$$d = \frac{a}{\sqrt{h^2 + k^2 + l^w}} \,, \tag{3}$$

where h, k and l are the Miller indices.

Miller indices (hkl) are used to describe a set of crystal planes (Barrett and Massalski [1]chapter 1; Kittel [3] chapter 1). The h, k, l are the reciprocal intercepts between a crystal plane and the lattice vectors in a unit cell. The distance between crystal planes is the interplanar distance d_{hkl}. The random orientation of large number of grains enables almost all (hkl) planes being observed as diffraction peaks.

However, reflections from some of the planes (h, k, l) do not occur when the crystal has additional symmetry beyond that of the simple cubic lattice. For face-centred cubic structures, reflections are mission if h, k and l are mixed odd and even. For body-centred cubic structures, reflections are mission is $h+k+l$ is odd (Barrett and Massalski [1] chapters 4, 7). Exceptions to the above correspond to variations in scattering power between atomic planes: differences in the atomic form factor (Barrett and Massalski [1] chapter 4).

The crystal lattice, defined by lattice vectors $\vec{a}$, $\vec{b}$ and $\vec{c}$, is a mathematical description of points in space arranged as the periodic array of atoms in a crystal. One or more atoms can be the basis that forms this array. The lattice has translational symmetry and other symmetries depending on the unit cell [2]. The magnitudes of the lattice vectors are called lattice constants a, b, and c and the angles formed by the lattice vectors are α, β, and γ.

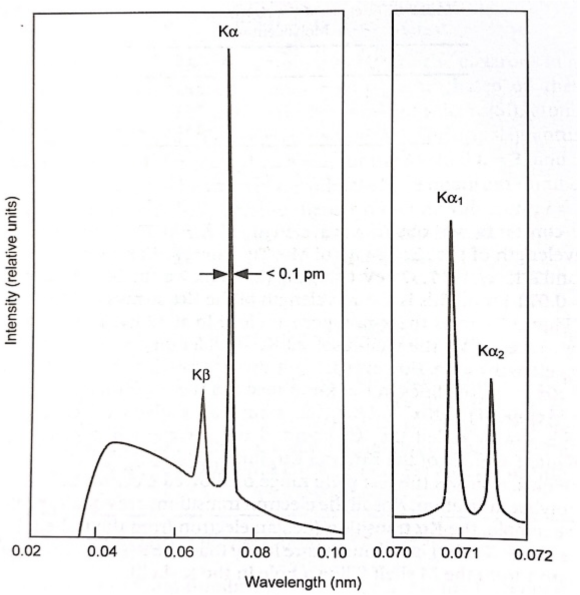

Figure 4: X-ray spectrum of Mo target at $35kV$, the expanded scale on the right shows the resolved $K\alpha_1$ and $K\alpha_2$ lines. The position of the peaks depends on the target element, e.g. Cu, Mo, W, ...

There are seven crystal systems in three dimensions with defined by different unit cell lattice constants and angles. [4].

If the crystals in the powder or the grains of the polycrystalline sample are too large there will be too few of them to span the full range of different orientations and the rings will therefore appear spotty. Rotating the sample can bring more crystal planes into orientations that satisfy Bragg's Law. If the grains are too small, the peaks will be broadened. The peak width and position shift give information on the size distribution and lattice strain inside the crystals [5].

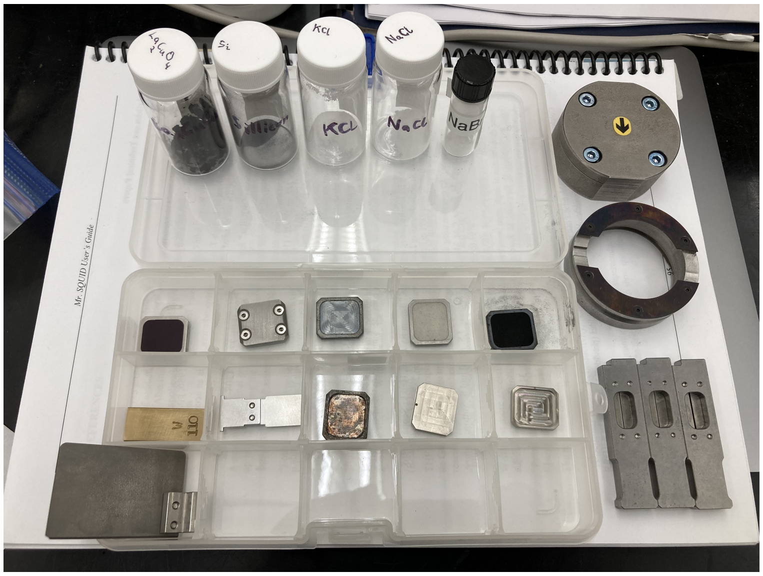

Figure 5: Required materials: Five powder samples in bottles, heating stage sample holders in the box with knife edges. The standard calibration slit block, single sample holder and three divergence slits on the left.

Safety Reminder

- Any student doing this experiment must wear a radiation dosimeter. These may be obtained from the APL technologists in MP 234. Dosimeters are not to be taken home, but returned to Room 234.
- If any sparking is seen or heard, if there is any unusual smell or noise, or any leakage is observed, all power to the apparatus should be turned off and a Professor or Technologist consulted.
- Be aware of the location of X-ray primary beam.
- Always wear a mask during sample loading to avoid inhaling the samples.
- Do not open the cabinet during X-ray operation.
- Use caution when operating the heating stage.
  - The stage can reach close to $500°C$, which is hot enough to burn your hand very badly, very quickly.
  - The stage does not cool instantaneously! Do not touch the stage until you are sure it is cool enough to easily handle.
  - Be aware of the melting point of the sample that you are investigating. Do not overheat the sample otherwise the heating stage and the sample holder may be damaged.
  - Be sure no flammable materials are in the vicinity of the stage. It can ignite many common materials, e.g. paper (ignition temperature $\sim 233°C$ or $451°F$), cotton ($\sim 250°C$), polyethylene ($\sim 349°C$), ethanol ($\sim 365°C$), ...
- Do not attempt to unplug the high-voltage power supply.
- Do not attempt to exceed the maximum voltage and current ratings for the X-ray tube.

NOTE: *This is not a complete list of all hazards; we cannot warn against every possible dangerous stupidity, e.g. opening plugged-in electrical equipment, juggling cryostats, etc. Experimenters must constantly use common sense to assess and avoid risks, e.g. if you spill liquid on the floor it will become slippery, sharp edges may cut you, etc. If you are unsure whether something is safe, ask the supervising professor, the lab technologist, or the lab coordinator. If an accident or incident happens, you must let us know. More safety information is available at* `http://www.ehs.utoronto.ca/resources.htm`.

4 Experiment Procedure

The Proto AXRD® Benchtop Powder X-ray Diffractometer Quick Start, Hardware, Software, and Analysis manuals (available on the PXR computer) are the primary resources for operating the instrument. It is recommended you start by with the Quick Start Guide, but here is a basic workflow.

1. Turn on the power (blue light). Insert key and rotate clockwise. Press the X-ray enable (green light).
2. Turn on the XRD software. Initialize Motor so that $\theta = 2\theta = 0$. Warm-up the X-ray tube for $7min$.
3. Finish alignment (in the order of θ_0 coarse, θ_0 fine, $2\theta_0$ coarse, $2\theta_0$ fine) procedure every time you turn on the machine and/or restart the software.
4. Prepare the sample so that its surface is flat. Place sample in a single sample holder (room temperature) or inside a heating stage.
5. Set the scanning parameters, i.e. θ, time, mode, etc.
6. Export .xye file, .png image and .xml file for further analysis.
7. When the scan is completed, disable the X-ray enable button, remove the key bby rotating counterclockwise, shut down the power, and close the software. Return the dosimeter and key.

4.1 Alignment

Most of the alignment procedure was done during the installation of the equipment, except for the goniometer zero angle θ_0 and $2\theta_0$ alignment. To do these, insert the slit block associated with the sample holder, align the arrow with the direction of the X-ray beam. Insert the $1.0mm$ divergence slit. In the alignment tab of the software, start with θ coarse alignment. Use Gaussian fit to locate the center of the peak, enter the location of peak into the software then move the motor to this new position. Record the fitting result the old/new count for later reference.

4.2 Heating stage

Reminder: The heating stage can get extremely hot! Be aware of the melting point of the sample that you are investigating. Do not overheat the sample otherwise the heating stage and the sample holder may be damaged.

The heating stage (BTS500) can heat samples from ambient temperature ($25°C$) to almost $500°C$. This allows studies of phase changes in materials that have transition temperatures in this range. Do not use the heating stage until you have made multiple measurements at room temperature and are confident in your ability to operate the diffractometer. The primary reference for the heating stage is the Anton-Parr Nambicon (Non-AMBient-CONtrol Software) Instruction Manual available on the instrument computer, but here is the basic workflow:

1. Open Nambicon software, create setpoint and hold time in the work sequence, save the file for later use.
2. Remove the single sample holder from the goniometer.
3. Check the O-rings are in place and tight and no contamination on the orange foil. [If replacement is necessary, refer to appendix.]
4. Carefully install the heating stage to the goniometer. Turn on the cabinet light if necessary.
5. Before plugging in the USB cable and power cable, start the alignment procedure. Make sure the slit block for heating stage is inserted.
6. Refer to the alignment tab in XRD software, start with θ coarse alignment. If a Gaussian peak is not found, then reinstall the heating stage (The stage need to be installed properly to ensure alignment procedure is not off by too much).
7. Finish the alignment procedure.
8. Load in powder samples into the holder, ensure the surface is flat. Deeper samples ($0.8mm$) usually yield better results. [number on the side]
9. Connect the power cable and the USB cable to the machine.
10. Load in the work sequence file to Nambicon. Connect the software with the heating stage.
11. Start the heating cycle. A typical temperature vs time is shown in Figure 7.

The measured temperature may need calibration using a powder with known thermal expansion, e.g. silicon powder as shown in Figure 7.

4.3 Data Acquisition Tips

Try to plan ahead your experiment to collect data in separate batch so that the consistency is preserved, i.e. avoid frequent calibration, start from room temperature gradually up to high temperatures. Rock salt must be prepared fresh to avoid moisture.

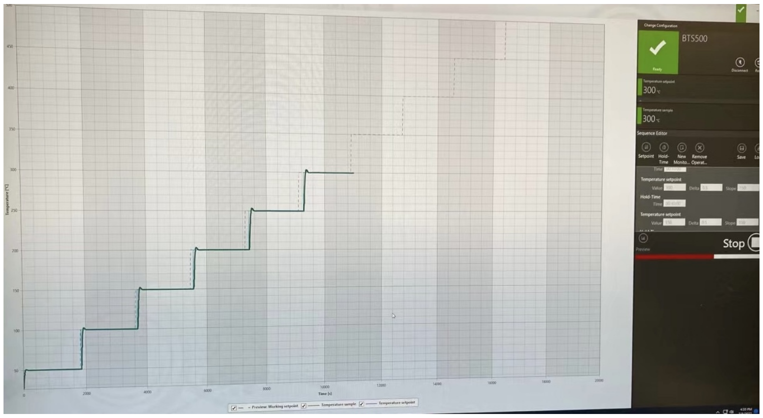

Figure 6: Work sequence for the heating stage. Notice that the delta and slope are causing delay in every cycle to ensure the temperature fluctuation is controlled.

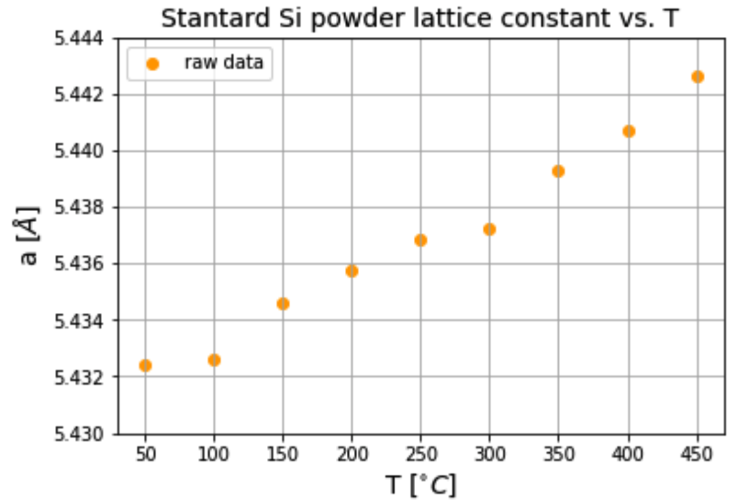

Figure 7: Temperature calibration curve for Silicon powder

5 Data Analysis

5.1 Indexing peaks

From the diffraction raw data, peak locations and relative intensities can be used to determine crystal structures. Precise lattice parameters can be calculated using Rietveld refinement, which is a least squares fitting method between the experimental data and a diffraction pattern calculated from a compound with the composition and crystal structure specified.

Cohen Analytical Method

Cubic structure is the simplest case with the minimum number of parameters.

$$\begin{aligned} \frac{1}{d_{hkl}} &= \frac{h^2+k^2+l^2}{a^2} \\ &= \frac{4sin^2\theta}{\lambda^2} \end{aligned} \tag{4}$$

$$sin^2\theta_{true} = \frac{\lambda^2}{4a_0^2}(h^2+k^2+l^2) \tag{5}$$

$$sin^2\theta_{observed} - sin^2\theta_{true} = \Delta sin^2\theta \tag{6}$$

Extrapolation

This method is only valid when the diffration peaks are located at high angle ($2\theta \geq 120°$). The linear Nelson-Riley function is extrapolated to get a_0 at $\theta_0 = 0$.

A GSAS II - Data Analysis Program

GSAS II software is a powerful tool to analyze powder diffraction data in a systematic way: Import data, background subtraction, 3 rounds of refinement, produce publish-level plots, etc. For install instructions and tutorials, please visit `https://subversion.xray.aps.anl.gov/trac/pyGSAS`. Some knowledge in point-symmetry group is required in creating phase files in GSAS II, please refer to [6].

References

[1] C. S. Barrett. *Structure of metals; crystallographic methods, principles, and data [by] Charles S. Barrett [and] T.B. Massalski.* McGraw-Hill series in materials science and engineering. McGraw-Hill, New York, 3d ed. edition (1966).

[2] Neil W. Ashcroft. *Solid state physics.* Saunders College, Philadelphia (1976). ISBN 978-0-03-049346-1.

[3] Charles Kittel. *Introduction to solid state physics.* Wiley, New York, 6th ed. edition (1986). ISBN 978-0-471-87474-4.

[4] Raja M. V. Pavan and Andrew R. Barron. “7.1 Crystal Structure”. In *Physical Methods in Chemistry and Nano Science.* Rice University (2016). URL `https://chem.libretexts.org/Bookshelves/Analytical_Chemistry/Physical_Methods_in_Chemistry_and_Nano_Science_(Barron)/07%3A_Molecular_and_Solid_State_Structure/7.01%3A_Crystal_Structure`.

[5] A. Khorsand Zak, W.H. Abd. Majid, M.E. Abrishami, and Ramin Yousefi. "X-ray analysis of ZnO nanoparticles by Williamson–Hall and size–strain plot methods". *Solid State Sciences*, 13(1):251–256 (2011). ISSN 12932558. doi:10.1016/j.solidstatesciences.2010.11.024. URL https://linkinghub.elsevier.com/retrieve/pii/S1293255810004607.

[6] Michael Tinkham. *Group Theory and Quantum Mechanics*. Dover Publications (2012). ISBN 978-1-306-34077-9. OCLC: 868270192.